CO oxidation mechanism of silver-substituted Mo/Cu CO-dehydrogenase. Analogies and differences to the native enzyme

Anna Rovaletti [*§] Giorgio Moro [†] Ugo Cosentino[*]
Ulf Ryde[‡] Claudio Greco[*§]

Abstract

The aerobic oxidation of carbon monoxide to carbon dioxide is catalysed by the Mo/Cu-containing CO-dehydrogenase enzyme in the soil bacterium *Oligotropha carboxidovorans*, enabling the organism to grow on the small gas molecule as carbon and energy source. It was shown experimentally that silver can be substituted for copper in the active site of Mo/Cu CODH to yield a functional enzyme. In this study, we employed QM/MM calculations to investigate whether the reaction mechanism of the silver-substituted enzyme is similar to that of the native enzyme. Our results suggest that the Ag-substituted enzyme can oxidize CO and release CO_2 following the same reaction steps as the native enzyme, with a computed rate-limiting step of 10.4 kcal/mol, consistent with experimental findings. Surprisingly, lower activation energies for C–O bond formation have been found in the presence of silver. Furthermore, comparison of rate constants for reduction of copper- and silver-containing enzymes suggests a discrepancy in the transition state stabilization upon silver substitution. We also evaluated the effects that differences in the water-active site interaction may exert on the overall energy profile of catalysis. Finally, the formation of a thiocarbonate intermediate along the catalytic pathway was found to be energetically unfavorable for the Ag-substituted enzyme. This finding aligns with the hypothesis proposed for the wild-type form, suggesting that the creation of such species may not be necessary for the enzymatic catalysis of CO oxidation.

[*]Department of Earth and Environmental Sciences, Milano-Bicocca University, Piazza della Scienza 1, Milano, 20126, Italy

[†]Department of Biotechnology and Biosciences, Milano-Bicocca University, Piazza della Scienza 2, Milano, 20126, Italy

[‡]Department of Theoretical Chemistry, Lund University, Chemical Centre, P.O. Box 124, SE-221 00 Lund, Sweden

[§]Corresponding authors

Keywords

Mo/Cu CO dehydrogenase, Ag catalyst, CO oxidation, nucleophilic addition, biocatalysis, entropy

1 Introduction

Carbon monoxide represents a trace gas in the atmosphere, whose presence derives both from natural and anthropogenic emissions. Nevertheless, some microbes base their autotrophic metabolism on such trace levels by exploiting oxidation reactions of CO.[1] Microbial CO metabolism is quite important to life on Earth, since about two hundred million tons of CO are removed from the lower atmosphere through bacterial oxidation every year, thus helping to maintain CO concentration below toxic levels.[2, 3] Aerobic CO oxidation is performed by carboxydotrophic bacteria that can use CO as their sole source of carbon and energy. In fact, the organisms grow autotrophically on carbon monoxide by coupling CO oxidation, performed by a particular metalloenzyme named Mo/Cu CO-dehydrogenase (MoCu-CODH), to CO_2 fixation into cell carbon through the Calvin–Benson–Basham pathway.[4, 5]

The most studied example of MoCu-CODH comes from the aerobic soil bacterium *Oligotropha carboxidovorans*. MoCu-CODH presents a symmetrical structure that is a dimer of heterotrimers $(\alpha\beta\gamma)_2$.[6] Each of its halves can be divided into three subunits: a larger subunit containing the active site (CoxL), a medium-sized subunit containing one FAD molecule (CoxM) and a smaller subunit containing two iron–sulfur centers [2Fe-2S] (CoxS).

The active site architecture of MoCu-CODH is constituted of a unique $MoO_2(\mu S)Cu$ bimetallic centre in the oxidised form of the enzyme.[7] The metal center of molybdenum is characterized by a pyramidal geometry with a distorted square base. The equatorial plane contains an oxo ligand, two sulfur atoms belonging to the molybdopterin cytosine dinucleotide (MCD) cofactor and a further sulfur atom acting as a bridge between molybdenum and copper ions (see Figure 1). In the apical position, a second oxo ligand is located. A second sulfur atom belonging to a cysteine residue (Cys388) is coordinated to the copper ion which connects the active site to the protein matrix.

In the second coordination sphere of molybdenum, a glutamate residue (Glu763) is located near the equatorial oxo ligand. Glu763 represents a highly conserved residue in the enzymatic family of xanthine oxidase, of which MoCu-CODH is a member. The hypothesis has recently been advanced that this residue plays a spectator role during the initial phase of the CO oxidation catalysis and then directly intervenes in the release of the CO_2 product.[8]

The bimetallic active site of the enzyme in its oxidized form hosts a molybdenum(VI) ion accepting electrons and a copper(I) ion capable of coordinating the CO substrate. During catalysis, Mo(VI) is reduced to Mo(IV), while Cu(I) maintains its oxidation state, thanks to the high degree of delocalisation within the Mo(μ-S)Cu unit.[6, 7, 9]

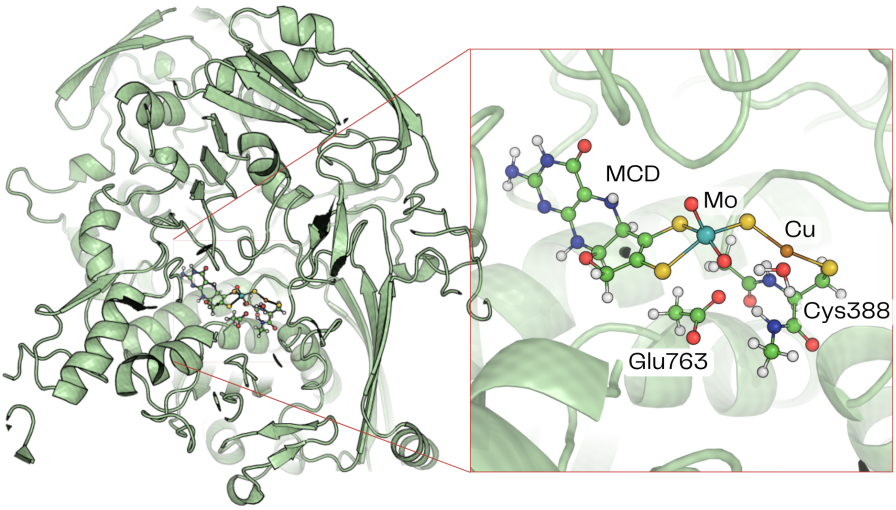

Figure 1: MoCu-CODH large subunit containing the active site (left) and a closer look at the bimetallic center (right). Colour code: Mo, cyan; Cu, orange; S, yellow; O, red; N, blue; C, green; H, white.

Under suitable conditions, the copper ion of the bimetallic site of CO-dehydrogenase can be replaced with silver.[10] The resulting enzyme has been found to maintain the ability to oxidise carbon monoxide. However, the Cu-to-Ag replacement results in a decrease in the CO-oxidation activity. At pH 7.2 and room temperature, the reported kinetic constants are 51 s^{-1} for MoCu-CODH and 8.1 s^{-1} for MoAg-CODH. Both catalysts follow pseudo first-order kinetics and the reaction rates are independent of the carbon monoxide concentration. Furthermore, the similarities of the EPR spectra of MoAg and the *wild-type* CODH imply a structural conformity of their active sites and their coordination spheres with the only exception of a water molecule that is found not to be coordinated to the Ag ion in the resting state of MoAg-CODH.[11] Overall, the aforementioned results suggest that silver-substituted CO-dehydrogenase adopts a catalytic mechanism quite similar to that of the native enzyme.

Over the past twenty years, many of several experimental and theoretical studies have been dedicated to understanding the mechanism of CO oxidation by MoCu-CODH.[12, 13] Crystallographic studies conducted on the enzyme have led to the hypothesis that the reaction mechanism involves the formation of a thiocarbonate intermediate. This is supported by the analogy of this structure with that assumed by the enzyme following irreversible inhibition by means of *n*-butylisocyanate.[6] Subsequent theoretical studies suggested that formation of the thiocarbonate species involves some difficulties in the evolution of the CO_2 product.[14] More recent studies [8] have presented a reaction mechanism for the oxidation of CO to CO_2 in good agreement with experimental data, in which the dissociation of carbon dioxide occurs directly from the product of the

nucleophilic attack, aided by temporary coordination of a carboxylate oxygen atom of Glu763 to the Mo ion and in which formation of the thiocarbonate intermediate does not constitute an obstacle for the enzymatic process.

In the present work, the energy profile for the Ag-substituted form of the enzyme was investigated, according to the catalytic mechanism recently suggested based on theoretical investigations in our laboratories for the *wild-type* enzyme.[8] The results obtained will also be discussed in comparative terms with respect to those obtained in the case of the copper-containing enzyme, leading to novel insights on the CO oxidation mechanism.

2 Results and Discussion

2.1 CO-to-CO_2 oxidation mechanism by MoAg-CODH

Unless otherwise stated, all energy differences discussed in the following refer to QM/MM refined energies computed by the BigQM approach at the B3LYP-D3(BJ)/def2-TZVPD level, as explained in the Methods section. As in the most recently reported CO oxidation catalytic mechanism [8], the first reaction step in the presence of silver consists of the nucleophilic attack of the equatorial oxygen of molybdenum on the C atom of carbon monoxide coordinated to the monovalent metal ion, resulting in the formation of a five-membered ring (see Figure 2). In the reactant species (**2Ag**), the CO molecule is coordinated to the silver ion and it is located in the same plane as the equatorial ligands of the molybdenum ion, with a O(Mo=O_{eq})–C(CO) distance of 2.24 Å. The reaction product **3Ag** is –4.5 kcal mol^{-1} more stable than **2Ag** and has a C–O bond length of 1.32 Å. The activation energy for the formation of the new C–O bond is 2.7 kcal mol^{-1}. In the transition state **TS-Ag** structure, the C–O distance of the forming bond is 1.83 Å.

The catalysis proceeds with the detachment of carbon dioxide from the active site starting from **3Ag**. During this reaction, simultaneous cleavage of the Mo–O(CO_2) and Ag–O(CO_2) bonds is observed, supported by the formation of a temporary interaction between one of the carbonyl oxygens of the glutamate residue (Glu763) and the molybdenum ion. In **3Ag**, the Mo–O(CO_2) and Ag–O(CO_2) bond lengths are 1.98 Å and 2.15 Å, respectively, and the Mo–O(Glu763) distance is 3.20 Å. The former distances increase to 2.32 Å and 2.94 Å in the transition state, **TS2-Ag**, while Mo–O(Glu763) decreases to 2.40 Å (see Figure 2). In the **4Ag** product, the CO_2 molecule is completely detached from the bimetallic core, with Mo–O(CO_2) and Ag–C(CO_2) distances of 2.60 Å and 3.14 Å, respectively. Glu763 is coordinated to the molybdenum ion, with a Mo–O(Glu763) distance of 2.26 Å. The CO_2 releasing step has an activation energy of 10.4 kcal mol^{-1}, but the resulting product **4Ag** is quite unstable (10.3 kcal mol^{-1} less stable than **3Ag**). A more stable product, **5Ag** (18.1 kcal mol^{-1} more stable than **4Ag**), is formed upon coordination of a water molecule to Mo, forming the Mo(IV)O(OH_2) reduced enzyme form. The water molecule coordinates at the empty equatorial position, with decoordination of the

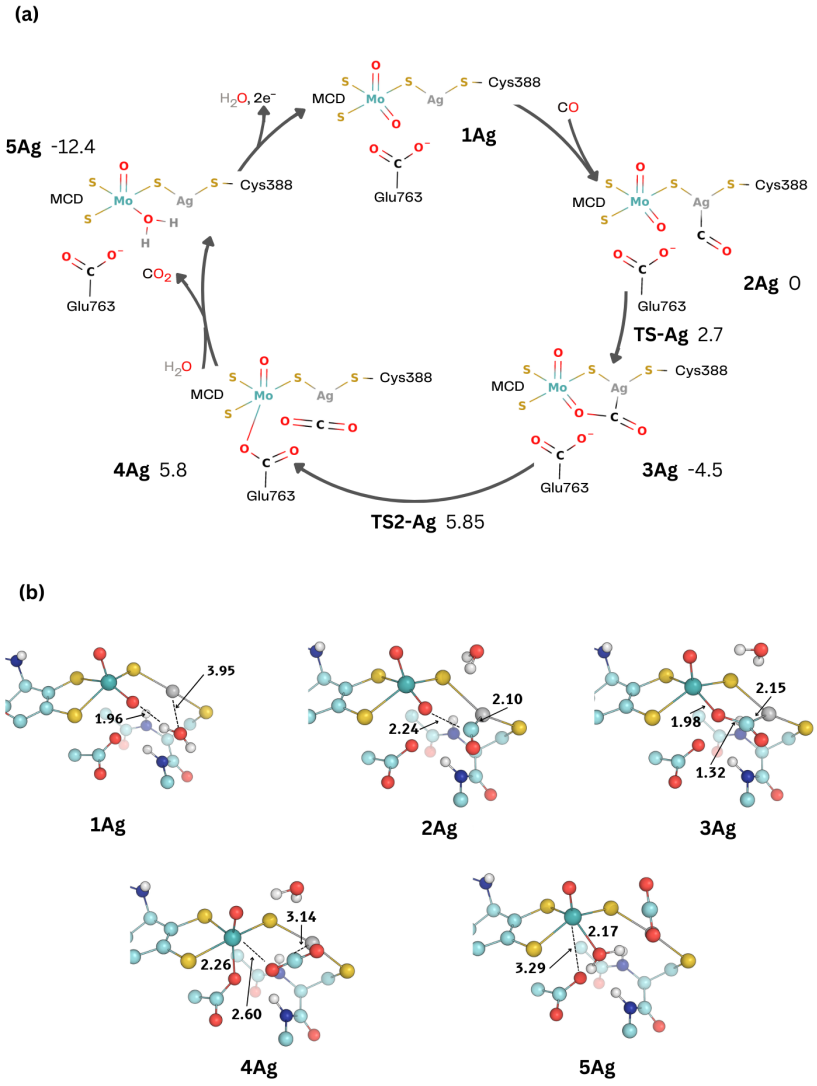

Figure 2: (a) Proposed catalytic cycle for the CO-to-CO_2 oxidation reaction by the MoAg-CODH enzyme. Relative energies with respect to the **2Ag** species are reported in kcal mol^{-1}. (b) Graphical representation of the optimised intermediates shown as balls and sticks. Non-polar hydrogens are omitted for clarity. Colour code: Mo, cyan; Ag, silver; S, yellow; O, red; N, blue; C, light blue; H, white. Distances are reported in Å.

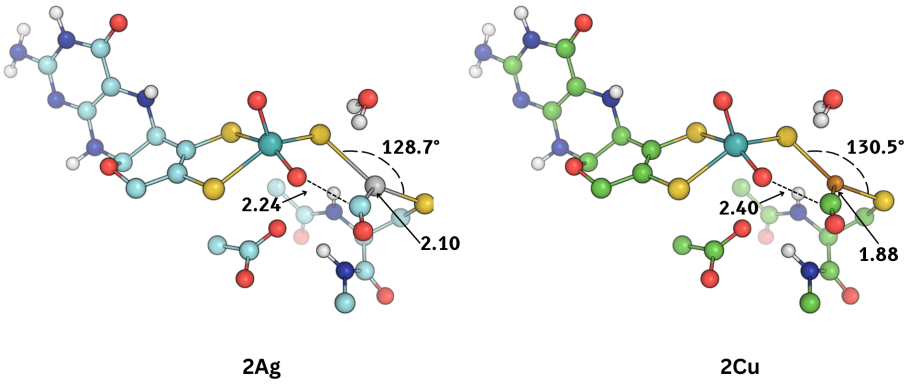

Figure 3: Graphical representation of the optimised intermediates **2Ag** and **2Cu**. Colour code for **2Ag** as in Figure 2. Color code for **2Cu** Mo, cyan; Cu, copper; S, yellow; O, red; N, blue; C, green; H, white. The most representative distances are reported in Å.

glutamate residue (the Mo–O(Glu763) distance is 3.29 Å and the Mo–O(H_2O) is 2.17 Å in **5Ag**).

2.2 Comparison between the CO oxidation mechanisms catalysed by MoAg-CODH and the *wild-type* enzyme

Next, we compared the optimised geometries of intermediates and transition states of the MoAg-CODH catalytic cycle and the associated energies with the corresponding results for the Cu-containing enzyme.[8] Replacement of the silver ion with copper leads to a decrease in the activation barrier for the nucleophilic attack reaction of the oxygen atom of the Mo=O_{eq} unit on the activated CO carbon. This activation energy is 6.9 kcal mol^{-1} for the MoCu-CODH enzyme and 2.7 kcal mol^{-1} for the Ag-substituted form. This is probably caused by the geometry of the intermediate **2Ag** (see Figure 3): the M–C(CO) distances is 1.88 Å for Cu but 2.10 Å for Ag in the optimised geometries of **2Cu** and **2Ag**, respectively. At the same time, the orientation of the carbon atom of the CO molecule is more favourable towards a nucleophilic attack by the equatorial oxo ligand of Mo in **2Ag** compared to what is observed in the copper-containing analogue (**2Cu**). In fact, the O_{eq}–C(CO) bond distance is appreciably shorter for Ag than for Cu (2.24 Å vs 2.40 Å).

In Ag-substituted CODH, the interaction of the glutamate residue with the molybdenum ion compensates for the removal of CO_2 and the subsequent decrease in the coordination number of the metal centre in the same way as

observed in the native enzyme (the Mo–O(Glu763) distance of TS2 is 2.29 Å for Cu and 2.40 Å for **TS2-Ag)**. For both enzymes, the rate-determining steps are in good agreement with the experimental data. In fact, the calculated activation energies of 12.6 kcal mol^{-1} for MoCu-CODH and 10.4 kcal mol^{-1} for MoAg-CODH show a good agreement with the experimentally determined activation enthalpies of 11.4 kcal mol^{-1} and 10.2 kcal mol^{-1}.[11]

In order to compare the complete catalytic cycle of CO oxidation of the *wild-type* and silver-substituted enzymes, binding energies of the CO substrate to the metal ion (Cu(I) or Ag(I)) were evaluated. The binding energy was calculated as explained in the Methods. Formation of the bond between carbon monoxide and M(I) is an exothermic reaction for both enzymes. As expected, Ag establishes a weaker interaction with CO; the calculated coordination energy was found to be 5.7 kcal mol^{-1} more favourable for copper. This is also in line with previous observations in literature that refer to a decrease in the π-backdonation capacity of Ag compared to Cu, which would be reflected in a lower activation of the CO substrate towards nucleophilic attack.[15] However, our results indicate that although the coordination of CO to Cu is actually more favourable than to Ag, the greater bulkiness of the silver ion leads to a spatial approach of the reacting species that favours the nucleophilic reaction. In other words, theory indicates that the effects of the lower π-backdonation capacity of Ag is counterbalanced by structural determinants that push the Ag-bound CO reactant closer to the product with the novel C–O bond.

2.3 Formation of the thiocarbonate intermediate during catalysis

As explained in the Introduction, the high thermodynamic stability of the thiocarbonate intermediate has sometimes been reported to be an obstacle in determining a plausible mechanism for the detaching of carbon dioxide. To complete the comparison between the two forms of the enzyme, the possible formation of the thiocarbonate intermediate during the course of catalysis in MoAg-CODH was evaluated. As shown in Figure 4, formation of the thiocarbonate intermediate occurs from **3Ag** by the formation of a bond between the carbon atom of the newly formed CO_2 moiety and the μ-sulfido ligand, concomitant with the breaking of the C–Ag bond, forming **6Ag**. After cleavage of the Ag–μS bond and formation of a (CO_2)O–Ag bond, the thiocarbonate intermediate **7Ag** is formed. Our calculations revealed that the silver-substituted structures are less stable than their native Cu-analogues. In particular, the incorporation of Ag as metal catalyst involves a significant loss of stability for the thiocarbonate intermediate (**7Ag**), which was found to be 8.7 kcal mol^{-1} less stable than **3Ag**, compared to 0.5 kcal mol^{-1} for the native enzyme. Assuming that substitution of Ag for Cu does not involve changes in the catalytic mechanism but only in the resulting kinetics, the high instability of the thiocarbonate compound as well as of its precursor intermediate further support the hypothesis suggested in the work of Ritacca *et al.* for the *wild-type* form[8] that the formation of such species is not necessary for the enzymatic catalysis of CO oxidation.

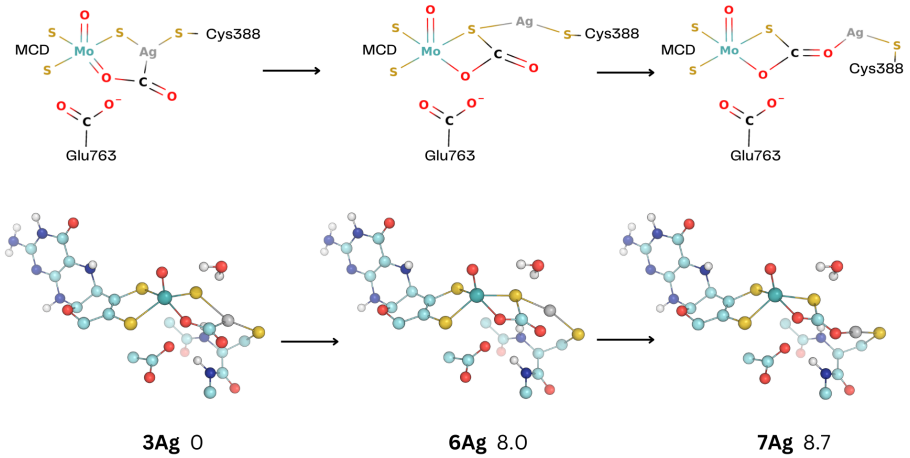

Figure 4: Graphical representation of the optimised intermediates involved in the formation of the thiocarbonate species. The numbers after the name of the intermediate is the relative stability in kcal mol^{-1}. Colour code as in Figure 2.

2.4 Entropic contributions

We saw above that the calculated activation energies for MoAg- and MoCu-CODH agree the experimental activation enthalpies within 0.2 and 1.2 kcal/mol and reproduce the trend of a lower activation enthalpy for Ag than for Cu. However, as mentioned in the Introduction, the reaction rate shows the opposite trend, *viz.* that k_{cat} is 8.1 and 51 s^{-1} for MoAg- and MoCu-CODH, respectively, translating to a difference in the activation free energy of 1.1 kcal/mol. This change must come from the entropic contributions and we investigate in this section such contributions. Reactions that lead to the formation of CO_2 once the substrate has been coordinated to the metal cation (**2Ag** $\rightarrow$ **3Ag** $\rightarrow$ **4Ag**, eqs. 2 and 3 for Ag and **2Cu** $\rightarrow$ **3Cu** $\rightarrow$ **4Cu**, eqs. 6 and 7 for Cu) are identical in the presence of either copper or silver. However, it is experimentally known that the resting states differ regarding whether a water molecule coordinates to the metal or not.[11] Therefore, it is reasonable to think that the energy profile associated with the catalytic processes in the Cu- and Ag-bearing enzymes can be significantly influenced by differences in entropic contribution coming from the CO bonding reaction (eqs. 1, 5) and from the reaction that leads to the formation of reduced enzyme state (eqs. 4, 8).

In particular, for MoCu-CODH, the net entropic contribution can be considered small because a gas molecule bound in eq. 5 is released in eq. 7 and concomitantly the water molecule released in eq. 5 binds again in eq. 8. However, this is not true for the silver-substituted enzyme, for which there is a cancelling entropy contribution deriving from the coordination of CO in eq. 1 and the

$$R_1{-}Mo(O){-}R_2{-}Ag + CO \rightleftharpoons R_1{-}Mo(O){-}R_2{-}Ag{-}CO \quad (1)$$

$$R_1{-}Mo(O){-}R_2{-}Ag{-}CO \rightleftharpoons R_1{-}Mo{-}R_2{-}Ag{-}CO_2 \quad (2)$$

$$R_1{-}Mo{-}R_2{-}Ag{-}CO_2 \rightleftharpoons R_1{-}Mo{-}R_2{-}Ag + CO_2 \quad (3)$$

$$R_1{-}Mo{-}R_2{-}Ag + H_2O \rightleftharpoons R_1{-}Mo(H_2O){-}R_2{-}Ag \quad (4)$$

Scheme 1: Chemical equations representing the CO-to-CO_2 oxidation catalysed by the silver-substituted enzyme: **1Ag** $\rightarrow$ **2Ag** (1); **2Ag** $\rightarrow$ **3Ag** (2); **3Ag** $\rightarrow$ **4Ag** (3) and **4Ag** $\rightarrow$ **5Ag** (4). R_1 represents the MCD and axial oxo ligand, R_2 represents the μS moiety and sulphur atom of Cys388 bound to Ag.

$$R_1{-}Mo(O){-}R_2{-}Cu{-}OH_2 + CO \rightleftharpoons R_1{-}Mo(O){-}R_2{-}Cu{-}CO + H_2O \quad (5)$$

$$R_1{-}Mo(O){-}R_2{-}Cu{-}CO \rightleftharpoons R_1{-}Mo{-}R_2{-}Cu{-}CO_2 \quad (6)$$

$$R_1{-}Mo{-}R_2{-}Cu{-}CO_2 \rightleftharpoons R_1{-}Mo{-}R_2{-}Cu + CO_2 \quad (7)$$

$$R_1{-}Mo{-}R_2{-}Cu + H_2O \rightleftharpoons R_1{-}Mo(H_2O){-}R_2{-}Cu \quad (8)$$

Scheme 2: Chemical equations representing the CO-to-CO_2 oxidation catalysed by the *wild-type* enzyme: **1Cu** $\rightarrow$ **2Cu** (5); **2Cu** $\rightarrow$ **3Cu** (6); **3Cu** $\rightarrow$ **4Cu** (7) and **4Cu** $\rightarrow$ **5Cu** (8). R_1 and R_2 are the same as for the silver enzyme.

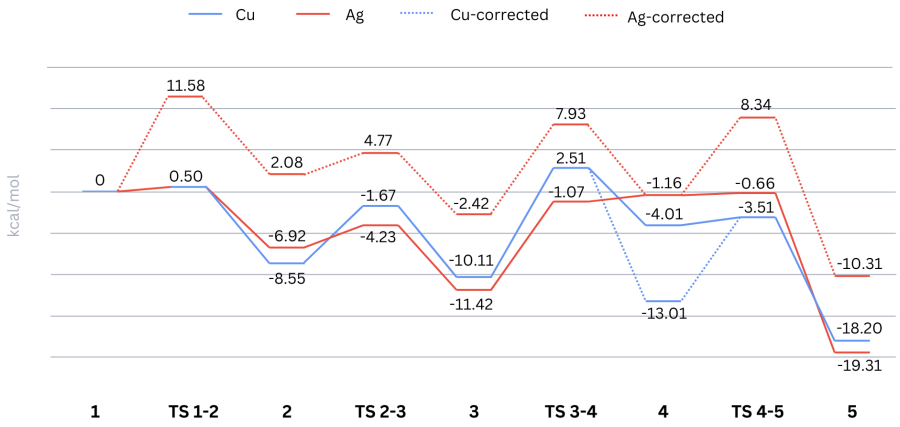

Figure 5: Potential energy surface of the CO-to-CO_2 oxidation mechanism catalysed by Mo/Cu-CODH (blue) and by Mo/Ag-CODH (red). Straight lines represent differences in total energies (ΔE) obtained by QM/MM calculations while dottet lines represent the approximated free-energies (ΔG) obtained by correcting the two-to-one particle QM/MM reactions energy by an entropic factor of 9.0 kcal/mol. All relative energies are expressed in kcal mol^{-1}.

release of CO_2 in eq. 3, but also an unfavourable entropic effect as a result of the coordination of the water molecule in eq. 4, which is not compensated by any release of water in eq. 1. In order to evaluate such entropic effects, the two-to-one particle reactions (eqs. 1, 3, 4, 7, 8) were corrected by an entropic factor of 9.0 kcal mol^{-1}, whose sign changes depending on whether the reaction implies an increase or not in entropy. Such a correction to ΔG (with ΔH approximated by ΔE) for any reaction step in which two molecules combine to form one has been used in many studies and it has little dependence on the molecular identity (8–11 kcal mol^{-1}) since the value is dominated by the translational and rotational entropy while the vibrational entropy, which depends more on the identity of the molecule, plays a secondary role.[16–20] We add the entropy factor to the transition states of binding reactions but not to dissociation reactions, because the ligand is (partly) bound in the transition state.

The approximated free-energy diagram is represented in Figure 5 and it is compared to the results obtained by only considering the total energy. It can be seen that the energies for MoCu-CODH is modified only for the **4** $\rightarrow$ **5** reaction, the barrier of which is increased, but the barrier remains lower than the rate-limiting **3** $\rightarrow$ **4** reaction (9.5 compared to 12.6 kcal mol^{-1}). However, for MoAg-CODH, most reaction steps are affected. In particular, the barrier for the **1** $\rightarrow$ **2** reaction step is increased to 11.6 kcal mol^{-1},which is actually higher than for the **3** $\rightarrow$ **4** step, which had the largest activation energy, 10.4 kcal mol^{-1}. This is not enough to reproduce the experimental free-energy trend, but it should be remembered that the entropy treatment is very primitive. In fact, an entropy correction of 11 kcal mol^{-1} gives the correct difference and it should be remembered that the calculated activation energy for MoCu-CODH was 1.2 kcal mol^{-1} higher than the experimental enthalpy. Moreover, vibrational entropy (and enthalpy) is ignored. Still, this simple model shows a possible explanation to the opposite trends of the activation energy and free energy. The results show striking resemblances between the total energy profiles of the *wild-type* enzyme and the Ag-substituted enzyme. Nevertheless, a notable divergence arises when entropy effects are taken into consideration. However, it is interesting to notice that such divergence is essentially neutral in terms of effects on the computed barrier for the CO_2 release steps, for which a good match with experimentally determined energies are noticed when the latter are compared with QM/MM-computed counterparts (*vide supra*).

3 Conclusions

Recent experiments performed by Wilcoxen *et al.* showed that silver can substitute for copper in the active site of MoCu-CODH to yield a functional enzyme.[10] Moreover, the EPR spectra indicated a coordination environment in the silver-substituted enzyme similar to that seen in the native form with the only exception that no proton coupling is observed in the presence of silver. This difference arises from the fact that a water molecule coordinates to the Cu ion, but not to Ag, in the resting state of the enzymes. In fact, it was suggested that a

Mo(VI)/Cu(I)–H_2O center is present in the *wild-type* form while a Mo(VI)/Ag(I) center is found in presence of silver.[11] The Ag-substituted enzyme preserves its ability to catalyse the oxidation of CO to CO_2 while the hydrogenases activity is completely lost with the introduction of the heavier metal.[11, 21]. Despite no catalytic mechanism for the CO-to-CO_2 oxidation by the MoAg-CODH form has been proposed so far, the identification of the rate-limiting step in the reductive half-reaction for both the native and Ag-substituted enzyme provides crucial insights into the mechanistic similarities between the two forms.[10] Therefore, in this work we used QM/MM calculations to investigate the possibility that the silver-substituted enzyme might follow the same mechanism as the native enzyme.[8]

Our results suggest that the silver-substituted enzyme can oxidise CO and release the CO_2 product following the same reaction steps reported for the native enzyme. A rate-limiting step of 10.4 kcal mol^{-1} was computed for the Ag-substituted form, which fits well to the experimentally reported one of 10.2 kcal mol^{-1}.[11] By comparing the CO-oxidation mechanism catalysed by MoAg-CODH with that of MoCu-CODH, a lower activation energy was found in the formation of the new C–O bond in the presence of silver. This intriguing finding contrasts with the expectation that silver, which is known to exhibit a lower π-backbonding capacity than copper, would result in a reduced activation of the C–O bond of the coordinated carbon monoxide.[15, 22] However, our results indicate that the more favourable C–O bond formation in the presence of Ag is not to be ascribed to a higher activation of the metal-bound CO molecule but to a more convenient position of the latter in the active-pocket site. In fact, we show that the bulkier silver ion pushes the CO molecule closer to the nucleophilic oxo ligand of Mo in contrast to what occurs in the presence of copper.

Regarding a comparison of the rate constants for reduction of the copper- and silver-containing enzyme, it was previously suggest that there is a discrepancy of approximately 1 kcal/mol in the transition state stabilisation upon substitution of silver for copper.[15] However, such difference is hard to assess with the current QM/MM enzyme modeling. Still, considering the outcomes derived from our model and the large effects due to differences in entropic contributions (*vide supra*, section 2.3), it is tempting to hypothesize that the rate difference between the two enzyme forms may be associated with such entropic effects.

Finally, formation of a thiocarbonate intermediate along the catalytic path turned out to be energetically unfavourable for the Ag-substituted enzyme. Assuming that the substitution of Cu for Ag does not entail alterations in the catalytic mechanism, the high instability of both the thiocarbonate compound and its precursor intermediate further reinforces the hypothesis proposed in the work of Ritacca *et al.* for the *wild-type* enzyme that the creation of such species is dispensable for the enzymatic catalysis of CO oxidation.[8]

Future studies in our laboratories will focus on assessing the impact of the selected Cu-to-Ag substitution on the catalytic energy profile of H_2 oxidation.

4 Computational Methods

4.1 QM/MM calculations

The protein setup reported in our previous work was used.[8] For the description of the structures of all the intermediates and transition states, the hybrid quantum mechanical/classical (QM/MM) approach has been employed. The protein and its surroundings were divided into two subsystems, called System 1 and System 2. System 1 comprises the active site of the enzyme and was treated by quantum mechanical calculations. It involved 66 atoms having a total charge of -3. It includes the molybdenum/silver bimetallic centre, carbon monoxide, the truncated MCD cofactor, the residue (Cys388) whose side chain coordinates Ag, the main chain of the two residues adjacent to this residue (Arg387–Ser389) and the side chain of the deprotonated glutamate residue (Glu763); finally, a water molecule of the second coordination sphere of silver was also included, the presence of which is known from crystallographic measurements carried out on the native enzyme.

System 2 comprises the remaining portion of the protein and a sphere of solvation water molecules. This subsystem was treated using a classical approach. In order to delimit System 1, the carbon atoms involved in the covalent bridging bonds between Systems 1 and 2 were treated by the hydrogen link-atom approach.[23] System 1 was capped with hydrogen atoms (hydrogen link atoms, HL) whose positions are linearly related to the corresponding carbon atoms (carbon link atoms, CL) in the full system.

QM/MM calculations were performed by means of the ComQum software,[24, 25] which uses a subtractive scheme with electrostatic embedding and van der Waals link-atom corrections.[26] All QM/MM geometric optimizations were performed on closed-shell singlet states at the BP86-D3(BJ)/def2-TZVP[27–30] level of theory using TURBOMOLE 7.4 software.[31] The resolution-of-identity technique was used to accelerate the calculations.[32]

For the MM calculations we used the Amber software,[33] using the Amber FF14SB force field for the protein,[34] and the general Amber force field[35] with restrained electrostatic potential (RESP) charges[36] for CO and the MCD cofactor. The two Fe_2S_2 clusters were described with RESP charges and a non-bonded model.[37]

The total energy of the QM/MM system is composed as follows:

$$E_{\mathrm{QM/MM}} = E^{\mathrm{HL}}_{\mathrm{QM1+ptch2}} + E^{\mathrm{CL}}_{\mathrm{MM12},q_1=0} - E^{\mathrm{HL}}_{\mathrm{MM1},q_1=0} \tag{9}$$

where $\mathrm{E}^{\mathrm{HL}}_{\mathrm{QM1+ptch2}}$ denotes the QM energy of System 1 truncated by HL atoms and embedded in a set of point charges modelling System 2. $\mathrm{E}^{\mathrm{HL}}_{\mathrm{MM1},q_1=0}$ is the MM energy of System 1, still truncated by HL atoms, without any electrostatic interactions. $\mathrm{E}^{\mathrm{CL}}_{\mathrm{MM12},q_1=0}$ is the classical energy of the whole system, with CL atoms and with the charges in System 1 set to zero, in order to avoid double-counting of the electrostatic interactions.

4.2 BigQM calculations

The BigQM approach was employed to obtain stable and converged energies of each optimised geometry in the CO-oxidation catalysis. This method[38, 39] has been shown to be a valuable tool in theoretical investigation of Mo/Cu CODH.[40, 41] The BigQM approach employs a QM system that includes all chemical groups with at least one atom within 6.0 Å of the original QM system of 66 atoms (System 1). In addition, junctions were moved three amino acids away from any residue in System 1 and all buried charged groups buried inside the protein were included, with exception of the two iron–sulfur clusters (Arg27, 30, 56, 112, 126, 138, 188, 211, 261, 301, 312, 387, 391, 418, 460, 571, 797; Asp30, 42, 43, 103, 124, 192, 266, 313, 338, 439, 507, 779, 794; Glu117, 218, 299, 394, 400, 404, 533, 555, 705, 714, 763; Lys60, 185, 274, 296, 379, 759; Hip532). The BigQM calculations were performed on coordinates obtained from the QM/MM optimisations, with a surrounding point-charge model, at the BP86-D3(BJ)/def2-SV(P) level.[42] The multipole accelerated resolution-of-identity J approach (marij keyword) was employed to accelerate the calculations.[43] The resulting energies were corrected with a QM/MM MM term for the BigQM region:

$$E_{\mathrm{MM}} = E^{\mathrm{CL}}_{\mathrm{MM12},q_1=0} - E^{\mathrm{HL}}_{\mathrm{MM1},q_1=0} \tag{10}$$

Finally, the energies were also corrected by taking into consideration the B3LYP-D3(BJ) functional and the def2-TZVPD basis set, using calculations with the standard QM/MM QM system and a point-charge model of the surroundings:

$$E_{\mathrm{corr}} = E^{\mathrm{B3LYP/TZVPD}}_{\mathrm{QM1,ptch2}} - E^{\mathrm{BP86/SV(P)}}_{\mathrm{QM1,ptch2}} \tag{11}$$

The CO binding energy was computed according to $\mathrm{M(I)} + \mathrm{CO_{aq}} \rightarrow \mathrm{M(I)\text{-}CO}$, where CO is considered as solvated in bulk water using the COSMO continuum solvent model (epsilon = 78).[44] M(I) was modelled with a QM/MM model whose System 1 was composed of 64 atoms while M(I)-CO was modelled using the standard QM/MM described above (System 1 composed of 66 atoms). All QM/MM energies were corrected using the Big-QM approach at the B3LYP-D3(BJ)/def2-TZVPD level of theory.

5 Acknowledgment

The computations were performed on computer resources provided by LUNARC, the Centre of Scientific and Technical Computing at Lund University, and on computer resources provided by CINECA as part of the agreement with the University of Milano-Bicocca.

6 Funding

This investigation has been supported by grants from the Swedish research council (projects 2018-05003 and 2022-04978).

7 Data availability statement

Raw data from the calculations are available from the corresponding author upon request.

8 Conflict of interest

The authors declare no conflict of interest.

References

(1) Robb, F. T.; Techtmann, S. M. *F1000Research* **2018**, *7*.

(2) Mörsdorf, G.; Frunzke, K.; Gadkari, D.; Meyer, O. *Biodegradation* **1992**, *3*, 61–82.

(3) Liu, L.; Zhuang, Q.; Zhu, Q.; Liu, S.; van Asperen, H.; Pihlatie, M. *Atmospheric Chemistry and Physics* **2018**, *18*, 7913.

(4) Ragsdale, S. W. *Critical reviews in biochemistry and molecular biology* **2004**, *39*, 165–195.

(5) Can, M.; Armstrong, F. A.; Ragsdale, S. W. *Chemical reviews* **2014**, *114*, 4149–4174.

(6) Dobbek, H.; Gremer, L.; Kiefersauer, R.; Huber, R.; Meyer, O. *Proceedings of the National Academy of Sciences* **2002**, *99*, 15971–15976.

(7) Gnida, M.; Ferner, R.; Gremer, L.; Meyer, O.; Meyer-Klaucke, W. *Biochemistry* **2003**, *42*, 222–230.

(8) Ritacca, A. G.; Rovaletti, A.; Moro, G.; Cosentino, U.; Ryde, U.; Sicilia, E.; Greco, C. *ACS Catalysis* **2022**, *12*, 7336–7343.

(9) Gourlay, C.; Nielsen, D. J.; White, J. M.; Knottenbelt, S. Z.; Kirk, M. L.; Young, C. G. *Journal of the American Chemical Society* **2006**, *128*, 2164–2165.

(10) Wilcoxen, J.; Snider, S.; Hille, R. *Journal of the American Chemical Society* **2011**, *133*, 12934–12936.

(11) Wilcoxen, J.; Hille, R. *Journal of Biological Chemistry* **2013**, *288*, 36052–36060.

(12) Hofmann, M.; Kassube, J. K.; Graf, T. *JBIC Journal of Biological Inorganic Chemistry* **2005**, *10*, 490–495.

(13) Kaufmann, P.; Duffus, B. R.; Teutloff, C.; Leimkühler, S. *Biochemistry* **2018**, *57*, 2889–2901.

(14) Rovaletti, A.; Bruschi, M.; Moro, G.; Cosentino, U.; Greco, C. *Frontiers in Chemistry* **2019**, *6*, 630.

(15) Hille, R.; Dingwall, S.; Wilcoxen, J. *JBIC Journal of Biological Inorganic Chemistry* **2015**, *20*, 243–251.

(16) Watson, L.; Eisenstein, O. *Journal of chemical education* **2002**, *79*, 1269.

(17) Thorhallsson, A. T.; Benediktsson, B.; Bjornsson, R. *Chemical Science* **2019**, *10*, 11110–11124.

(18) Siegbahn, P. E. *Physical Chemistry Chemical Physics* **2019**, *21*, 15747–15759.

(19) Wei, W.-J.; Siegbahn, P. E. *Chemistry–A European Journal* **2022**, *28*, e202103745.

(20) Jiang, H.; Ryde, U. *Dalton Transactions* **2023**.

(21) Rovaletti, A.; Bruschi, M.; Moro, G.; Cosentino, U.; Greco, C.; Ryde, U. *Inorganics* **2019**, *7*, 135.

(22) Antes, I.; Dapprich, S.; Frenking, G.; Schwerdtfeger, P. *Inorganic Chemistry* **1996**, *35*, 2089–2096.

(23) Reuter, N.; Dejaegere, A.; Maigret, B.; Karplus, M. *The Journal of Physical Chemistry A* **2000**, *104*, 1720–1735.

(24) Ryde, U. *J Comput Aid Mol Des* **1996**, *10*, 153–164.

(25) Ryde, U.; Olsson, M. H. *International Journal of Quantum Chemistry* **2001**, *81*, 335–347.

(26) Cao, L.; Ryde, U. *Frontiers in chemistry* **2018**, *6*, 89.

(27) Becke, A. D. *Physical review A* **1988**, *38*, 3098.

(28) Perdew, J. P. *Physical Review B* **1986**, *33*, 8822.

(29) Grimme, S.; Ehrlich, S.; Goerigk, L. *Journal of computational chemistry* **2011**, *32*, 1456–1465.

(30) Weigend, F.; Ahlrichs, R. *Physical Chemistry Chemical Physics* **2005**, *7*, 3297–3305.

(31) TURBOMOLE V7.1 2016, a development of University of Karlsruhe and Forschungszentrum Karlsruhe GmbH, 1989-2007, TURBOMOLE GmbH, since 2007; available from `http://www.turbomole.com`.

(32) Eichkorn, K.; Weigend, F.; Treutler, O.; Ahlrichs, R. *Theoretical Chemistry Accounts: Theory, Computation, and Modeling (Theoretica Chimica Acta)* **1997**, *97*, 119–124.

(33) Case, D.; Babin, V.; Berryman, J.; Betz, R.; Cai, Q.; Cerutti, D.; Cheatham Iii, T.; Darden, T.; Duke, R.; Gohlke, H., et al. **2014**.

(34) Maier, J. A.; Martinez, C.; Kasavajhala, K.; Wickstrom, L.; Hauser, K. E.; Simmerling, C. *Journal of chemical theory and computation* **2015**, *11*, 3696–3713.

(35) Wang, J.; Wolf, R. M.; Caldwell, J. W.; Kollman, P. A.; A., C. D. *J. Comput. Chem.* **2004**, *25*, 1157–1174.

(36) Bayly, C. I.; Cieplak, P.; Cornell, W. D.; Kollman, P. A. *J. Phys. Chem.* **1993**, *97*, 10269–10280.

(37) Hu, L.; Ryde, U. *J. Chem. Theory Comput.* **2011**, *y*, 2452–2463.

(38) Hu, L. H.; Söderhjelm, P.; Ryde, U. *J Chem Theory Comput* **2012**, *9*, 640–649.

(39) Sumner, S.; Söderhjelm, P.; Ryde, U. *J Chem Theory Comput* **2013**, *9*, 4205–4214.

(40) Rovaletti, A.; Bruschi, M.; Moro, G.; Cosentino, U.; Ryde, U.; Greco, C. *Journal of Catalysis* **2019**, *372*, 201–205.

(41) Rovaletti, A.; Greco, C.; Ryde, U. *Journal of Molecular Modeling* **2021**, *27*, 1–11.

(42) Schäfer, A.; Horn, H.; Ahlrichs, R. *The Journal of Chemical Physics* **1992**, *97*, 2571–2577.

(43) Sierka, M.; Hogekamp, A.; Ahlrichs, R. *The Journal of chemical physics* **2003**, *118*, 9136–9148.

(44) Klamt, A.; Schüürmann, G. *Journal of the Chemical Society, Perkin Transactions 2* **1993**, 799–805.

9 Table of Contents graphical abstract

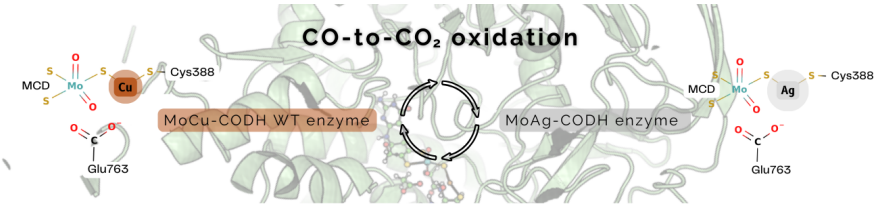

Figure 6: The catalytic CO-to-CO_2 oxidation mechanism by means of the Ag-substituted form of the MoCu CO dehydrogenase enzyme unravelled by means of theoretical investigations.